行政院國家科學委員會專題研究計畫 成果報告

大白鼠中腦 A7 核區正腎上腺素神經元 A 型鉀離子電流之分子和生理特性分析與角色探討(第 3 年)
研究成果報告(完整版)

計 畫 類 別 ：個別型
計 畫 編 號 ：NSC 95-2320-B-040-011-MY3
執 行 期 間 ：97 年 08 月 01 日至 99 年 07 月 31 日
執 行 單 位 ：中山醫學大學生物醫學科學學系（所）

計 畫 主 持 人：楊琇雯
共 同 主 持 人：閔明源

報 告 附 件 ：出席國際會議研究心得報告及發表論文

處 理 方 式 ：本計畫涉及專利或其他智慧財產權，2 年後可公開查詢

中 華 民 國 99 年 11 月 05 日

行政院國家科學委員會補助專題研究計畫 ☑ 成 果 報 告
□期中進度報告

大白鼠中腦 A7 核區正腎上腺素神經元 A 型鉀離子電流之分子和生理特性分析與角色探討

計畫類別：☑個別型計畫　□整合型計畫
計畫編號：NSC 95－2323－B－040－011－MY3
執行期間：2006 年 08 月 01 日至 2010 年 07 月 31 日

執行機構及系所：中山醫學大學 生物醫學科學系

計畫主持人：楊 琇 雯
共同主持人：閔 明 源

成果報告類型(依經費核定清單規定繳交)：□精簡報告　☑完整報告

本計畫除繳交成果報告外，另須繳交以下出國心得報告：
□赴國外出差或研習心得報告
□赴大陸地區出差或研習心得報告
☑出席國際學術會議心得報告
□國際合作研究計畫國外研究報告

處理方式：除列管計畫及下列情形者外，得立即公開查詢
□涉及專利或其他智慧財產權，□一年☑二年後可公開查詢

中　華　民　國　99　年 10 月 28 日

目 錄

壹、中文摘要

本計畫研究正腎上腺性 A7 神經元的膜電位依賴鉀離子電流(簡稱為鉀電流)的特徵。在正腎上腺性 A7 神經元所引發的鉀電流，包含有 A-型鉀電流(簡稱為 A 電流)，其特徵為具有較低的活化閾值(約-50 mV)，α快速的活化與去活化動力學特徵，與能快速的自去活化狀態回復。由於 A 電流此能被 heteropodatoxin-2 (Hptx-2)，此一 Kv4 通道的選擇性抑制劑所抑制，並且正腎上腺性 A7 神經元被證實對抗 Kv4.1/Kv4.3 通道蛋白的抗體具有免疫反應，我們結論在正腎上腺性 A7 神經元所引發的 A 電流是由 Kv4.1/Kv4.3 通道蛋白所媒介。以在 current-clamp 記錄模式中所記錄得的正腎上腺性 A7 神經元的單一動作電位波形，自主放電時兩個動作電位間的閾值下膜電位變化波形，與 EPSP 波形作為 voltage-clamp 記錄的膜電變化，作為 voltage-clamp 實驗的電位嵌定指令，也能在正腎上腺性 A7 神經元中引發 A 電流。在 current-clamp 記錄模式中，以 4-AP， 此一 A 電流抑制劑,或者 Hptx-2 抑制 A 電流後，造成動作電位的半輻寬與自主放電頻率的增加；此外，能引發細胞放射動作電位所需的突觸輸入強度則下降。綜合以上 voltage-clamp 記錄與 current-clamp 記錄結果，我們結論在正腎上腺性 A7 神經元所中，A 電流於調節動作電波形，放電頻率與突觸訊號整合上，扮演極重要角色。由於這群神經元主要投射到脊髓的背角，以上的結果也暗示，Kv4.1/Kv4.3 通道蛋白在下行性的腎上腺性止痛機轉上，扮演重要的角色。

關鍵詞: 4-AP; heteroprodotoxin-2; Kv4.1; Kv4.2; Kv4.3; 痛覺

貳、Abstract (英文摘要)

We investigated voltage-dependent K^+ currents (I_K) in noradrenergic (NAergic) A7 neurons. The I_K evoked consisted of A-type I_K (I_A), which had the characteristics of a low threshold for activation (~ -50 mV), fast activation/inactivation, and rapid recovery from inactivation. Since the I_A were blocked by heteropodatoxin-2 (Hptx-2), a specific Kv4 channel blocker, and the NAergic A7 neurons were shown to be reactive with antibodies against Kv4.1/Kv4.3 channel proteins, we conclude that the I_A evoked in NAergic neurons are mediated by Kv4.1/Kv4.3 channels. I_A were also evoked using voltage commands of a single action potential (AP), a subthreshold voltage change between 2 consecutive APs, or EPSP activity recorded in current-clamp mode (CCM). Blockade of the I_A by 4-AP, a broad spectrum I_A blocker, or by Hptx-2 increased the half-width and spontaneous firing of APs and reduced the amount of synaptic drive needed to elicit APs in CCM, showing that the I_A play important roles in regulating the shape and firing frequency of APs and in synaptic integration in NAergic A7 neurons. Since these neurons are the principal projection neurons to the dorsal horn of the spinal cord, these results also suggest roles for Kv4.1/4.3 channels in descending NAergic pain regulation.

Keywords: 4-AP; heteroprodotoxin-2; Kv4.1; Kv4.2; Kv4.3; pain

叁、報告內容：

本計畫成果已於 Neruoscience (2008)第 153 卷，1020-1033 頁與 Neruoscience (2010) 第 168 卷，633-645 頁發表，所以此一成果報告內容取於該 2 篇論文內容。

一、前言與文獻回顧

Morphological evidence suggests that the axonal terminals projecting from pontine noradrenergic (NAergic) neurons in the A7 catecholamine cell group, referred to as NAergic A7 neurons, are one of the principal sources of NAergic innervation in the dorsal horn of the spinal cord (Clark and Proudfit, 1991; Jones, 1991; Howorth et al., 2009). Since it has been clearly demonstrated that intrathecal (IT) injection of noradrenaline or α2-adrenoreceptor agonists produces a significant analgesic effect (Reddy and Yaksh, 1980; Kuraishi et al., 1985; Danzebrink and Gebhart, 1990; Takano and Yaksh, 1992), it is generally believed that NAergic A7 neurons play an important role in modulation of nociceptive signaling (Holden and Pizzi, 2003; Pertovaara, 2006). In support of this argument, direct electrical or chemical stimulation of NAergic A7 neurons results in significant analgesia (Hodge et al., 1986; Yeomans and Proundfit, 1992; Yeomans et al., 1992; Holden et al., 1999), which is blocked by IT administration of an α2-adrenoreceptor antagonist in rats (Takano and Yaksh, 1992; Yeomans et al., 1992; Holden et al., 1999). It is well established that electrical or chemical stimulation of descending inhibitory nuclei, such as the periaqueductal gray area (PAG), ventromedial medulla (VMM), or pedunculopontine tegmental (PPT) nucleus, produces profound analgesia (Millan, 1999, 2002), and, interestedly the extent of this has been shown to be largely reduced by IT administration of α-adrenoceptor antagonists in rats (Sagen and Proudfit, 1981; Satoh et al., 1983; Barbaro et al., 1985; Dias et al., 2009). Since there are no NAergic neurons in the PAG, VMM, PPT, or spinal cord (Carlsson et al., 1964; Dahlstörm and Fuse, 1964), these results suggest that the PAG, VMM, or PPT may exert some of their analgesic effect by modulating the excitability of NAergic A7 neurons (Holden and Pizzi, 2003). Nevertheless, the detailed cellular mechanisms underlying the analgesic effect caused by stimulating NAergic A7 neurons, either through their direct dorsal horn projection or by possible interaction with the PAG, PPT, and VMM, are poorly understood. To explore these mechanisms, full characterization of the firing and membrane properties of, and the underlying ionic mechanisms in, NAergic A7 neurons are necessary.

We have recently characterized the firing pattern and passive membrane properties of NAergic A7 neurons using the whole-cell variant of patch-clamp recording (Min et al., 2008). NAergic A7 neurons fire action potentials (APs) spontaneously, injection of a hyperpolarizing current pulse stops this spontaneous firing, and, when the current injection is turned off, there is a prominent delay in resumption of spontaneous firing (Min et al., 2008). Since similar physiological features have been reported in neurons that express high levels of Kv4 channel protein (Liss et al., 2001; Burdakov and Ashcroft, 2002; Burdakov et al., 2004), one of the putative pore-forming α-subunits of voltage-dependent K^+ channels that mediate fast activation and inactivation A-type voltage-dependent potassium currents (I_A) (Coetzee et al., 1999; Jerng e al., 2004a), we speculated that NAergic A7 neurons might express high levels of functional Kv4 channels. The I_A mediated by Kv4 channels has been shown to play important roles in governing spike shape, firing frequency, and synaptic integration and plasticity (Liss et al., 2001; Burdakov and Aschroft, 2002; Ramakers and Storm 2002; Burdakov et al., 2004; Chen et al., 2006; Hu et al., 2006). The aims of the present study were therefore to characterize the dynamic and pharmacological properties of the I_A and explore their possible functional role in the control of the discharge properties of NAergic A7 neurons.

二、實驗方法與材料

Animals and preparation of brainstem slices

Sprague-Dawley rat pups of both sexes, aged 7-10 days, were used in this study. The experimental protocols and use of animals were approved by the local Ethical Committee for Animal Research. All efforts were made to minimize the number of animals used and their suffering. Brainstem slices were prepared as described previously (Min et al., 2003). Briefly, the rat pups were decapitated and sagittal brainstem slices (300 μm thick), comprising the A7 area, trigeminal motor nucleus (Mo5), and surrounding regions, were cut with a vibroslicer (Dosaka, Tokyo , Japan). Slicing was perform in ice-cold artificial cerebrospinal fluid (ACSF) containing (in mM): NaCl 105, KCl 5, $MgSO_4$ 1.3, $NaHCO_3$ 24, NaH_2PO_4 1.2, $CaCl_2$ 2, and glucose 10, with the pH adjusted to 7.4 by gassing with 95% O_2/5% CO_2. The slices were kept in an interface-type chamber at room temperature (25-26°C) for at least 90 minutes to

allow recovery before start of recording.

Whole-cell recording of NAergic A7 neurons and electrophysiology

The slices were transferred to an immersion-typed recording chamber. Recordings were made from neurons with a large somatic diameter located about 200 μm rostral to the anterior border of Mo5 using patch pipettes pulled from borosilicate glass tubing (1.5 mm outer diameter, 0.5 mm wall thickness; Warner Instruments Corp., Hamden, CT, USA) and a patch amplifier (Multiclamp 700B; Axon Instruments Inc.; Union City, CA, USA) under an IR-DIC microscope (BX51WI, Olympus Optical Co., Ltd., Tokyo, Japan). The patch pipettes had a resistance of ~3 MΩ when filled with internal solution consisting of (in mM) potassium gluconate 116, potassium chloride 20, HEPES 10, sodium chloride 8, EGTA 2, biocytin 10, ATP 2, GTP 0.3; pH adjusted to 7.2 by KOH. The serial resistance was usually < 15M . and was compensated by at least 75%. The estimated junction potential was about 11 mV according to Neher (1992), and was corrected for during off-line analysis. Signals were low-pass filtered at a corner frequency of 2 kHz, then digitized at 10 kHz using a Micro 1401 interface (Cambridge Electronic Design, Cambridge, UK) running Signal software provided by CED. Leak subtraction was performed during off-line analysis.

Voltage-clamp recordings were made in ACSF to which 1 μM tetrodotoxin (TTX) was added and the extracellular Ca^{+2} replaced by equimolar Mg^{+2} or Cd^{+2} to block voltage-dependent Ca^{+2} and Na^{+} channels, respectively. In some experiments, 50 mM tetraethylammonium chloride (TEA) was added to the ACSF to block delay rectifier currents, the osmolarity being compensated by reducing the concentration of NaCl. The membrane voltage (Vm) was clamped at -70 mV, then whole-cell currents were evoked by applying sequential voltage pulses (duration: 1 s) stepping from a pre-pulse (duration: 0.5 s) of -90 mV to 0 mV, then stepping from a pre-pulse of -40 mV to 0 mV, this cycle being repeated every 3 s. The I_A were isolated by subtracting the current evoked by the -40 mV pre-pulse from that evoked by the -90 mV pre-pulse. To measure the reversal potential (E_r) of I_A, Vm was first stepped from -100 mV to 0 mV (duration: 5 ms), followed to a level ranging from -20 to -120 mV with 10 mV increments. The peak tail

currents were measured and a plot of I-V was constructed. The I-V plot was fitted with a quadratic polynomial (Bekkers, 2000). To measure voltage-dependent activation, a similar paradigm was employed, except that the voltage pulse was gradually stepped from -90 mV to +10 mV in 10 mV increments. The conductance of the I_A was calculated as:

$$G(V) = I(V)/(V - E_K)$$

where $G(V)$ is the conductance of the I_A with the Vm commanded to V, E_K the K^+ reversal potential (~-106 mV), and $I(V)$ the I_A peak amplitude. The activation curve was constructed by plotting V against $G(V)$ and was fitted to a fourth-order Boltzmann equation:

$$G(V) = A_0 / (1 + exp (-(V - V_{1/2}) / k))^4,$$

where V is the membrane potential, $V_{1/2}$ the potential at which half of the maximum conductance is achieved, k the slope factor, and A_0 a constant. To measure voltage-dependent inactivation, voltage pulses stepping from various levels of pre-pulse (-100 mV to -28 mV in 8 mV increments) to -25 mV were sequentially applied. The peak amplitudes of the I_A evoked by stepping from different pre-pulse levels were measured and normalized to the largest amplitude. The inactivation curve was constructed by plotting V against the normalized peak amplitude of the I_A and was fitted to the Boltzmann equation:

$$I(V) = A_0 / (1 + exp ((V - V_{1/2}) / k)) ,$$

where V is the membrane potential, $V_{1/2}$ the potential at which half of the peak I_A amplitude is achieved, k the slope factor, and A_0 a constant. To measure the time-dependent recovery from inactivation, two conditioning pulses with a duration of 0.8 s and stepped from -100 mV to -10 mV were applied. The inter-pulse interval was varied from 10 to 200 ms in increments of 10 ms. The recovery curve was constructed by plotting the inter-pulse interval against the peak amplitude of the I_A evoked by the 1st pulse divided by the peak amplitude of the I_A evoked by the 2nd pulse and was fitted to a single exponential function:

$$I(t) = A_0 + A_1 (1 – exp (-t / \tau)),$$

where $I(t)$ is the peak current ratio at the inter-pulse interval t and A_0 and A_1 are constants.

Elicitation of an excitatory postsynaptic potential (EPSP) or current (EPSC) in NAergic A7 neurons

was performed with a bipolar electrode placed near to the recorded neuron, with addition of 1 M strychnine and 100 mM picrotoxin to the bath to block inhibitory synaptic activity. A paired-pulse experiment was performed by application of two stimulating pulses separated by a 50 ms interval. For AP or EPSP-clamp experiments, recordings were first made in current-clamp mode (CCM) to record spontaneous APs or EPSP activity. The recordings were then switched to voltage-clamp mode (VCM), and the recorded AP, subthreshold voltage change between 2 consecutive APs of spontaneous firing, or EPSP activity (averaged from 100 consecutive single sweeps) was used as the voltage command for VCM recording. Membrane currents (I_m) evoked by AP or EPSP activity were first recorded in the control condition, then in the presence of 10 mM 4-aminopyridine (4-AP). The 4-AP-sensitive current was presumed to be the I_A and was obtained by subtracting the I_m recorded in 4-AP from that recorded in the control condition. To elicit an artificial EPSP (aEPSP), we positioned a patch pipette near the recorded neuron and applied 100 μM glutamate by air-puff (pressure: 3 - 10 psi; duration: 1 - 10 ms) to evoke an aEPSP in the recorded neuron. The aEPSP was first elicited in the control condition, then in the presence of 4-AP in the same neuron.

Unless specified, all data are expressed as the mean ± standard error of the mean and a one-way ANOVA-test or paired t-test was used for statistical comparison.

All drugs used were bath-applied. TEA, strychnine, and picrotoxin were purchased from Sigma, 4-AP from Tocris Cookson (Bristol, UK), and HpTx2, α-DTX (α-dendrotoxin), and BDS-I from Alomone Labs (Israel).

Immunohistochemistry for Kv4 channel labeling and post hoc NAergic A7 neurons identification

For Kv4 channel immunohistochemistry (IHC), the rats were deeply anesthetized by intraperitoneal (i.p.) injection with trichloroacetaldehyde monohydrate (10%) and perfused through the cardiovascular system with normal saline, followed by 4% paraformaldehyde in 0.1 M phosphate buffer (PB), pH 7.4. The brains were removed, postfixed in the same fixative for 4 h, and washed overnight at 4°C with PB.

Sagittal sections (50 m) were cut with a vibratome (Vibratome 1000, MO, USA) and incubated in 50 % alcohol in water for 30 minutes to increase membrane permeability to the antibodies used; this and all subsequent steps, unless otherwise stated, were at room temperature. After washing with water for 10 minutes, then with PB for 10 minutes, the sections were incubated with 0.5 % sodium borohydrate in PB for 30 minutes for antigen retrieval. Following a 10 minute wash with PB, the sections were incubated in phosphate-buffered saline (PBS) containing 0.01% Triton X-100, 10% normal goat serum, and 2% bovine serum albumin for 1 h to reduce non-specific binding of the antibodies. The sections were then incubated overnight at 4°C with either a mixture of rabbit anti-rat tyrosine hydroxylase (TH) antibodies (dilution:1/1000, Chemicon, Temecula, CA, USA) and mouse antibody against rat Kv4.1 or Kv4.2 channels (dilution:1/500, NeuroMab, University of California Davis, Davis, CA) or with a mixture of mouse antibody against PC12 cell TH (dilution: 1/1300; Chemicon, Temecula, CA, USA) and rabbit antibodies against human Kv4.1 channel (dilution: 1/100, Alomone Lab, Jerusalem, Israel). The sections were then washed and incubated for 2 h at room temperature with a mixture of TRITC-conjugated goat anti-mouse IgG and FITC-conjugated goat anti-rabbit IgG antibodies (both 1: 200; from Jackson). The sections were washed for 3 x 10 min with PBS between each incubation step. The results of staining were examined with a confocal microscope (Leica TCS SP5, Hamburger, Germany).

The recorded neurons were passively filled with biocytin and subjected to staining procedures similar to those described above, except that, after recording, the brainstem slices were immediately fixed overnight at 4°C with 4% paraformaldehyde (Merck, Frankfurt, Germany), then incubated overnight at 4°C with a mixture of AMCA-avidin D (dilution:1/250; Vector Laboratories, Burlingame, CA, USA) and mouse antibody against rat dopamine-β-hydroxylase (DBH) (dilution: 1/1300; Chemicon, Temecula, CA, USA), then for 2 h at room temperature with TRITC-conjugated goat anti-mouse IgG antibodies (Jackson). After staining, the recorded neuron were examined for DBH-immunoreactivity by conventional fluorescent microscopy (BX-50, Olympus, Tokyo, Japan).

三、結果

Isolation and properties of the I_A in DBH-ir neurons in the A7 area

Recordings were first made in current clamp mode (CCM) and depolarizing and hyperpolarizing current pulses were injected to check the firing and membrane properties of the recorded neurons. Only neurons that displayed previously reported electrophysiological properties of NAergic A7 neurons (Min et al., 2008), including no appearance of voltage sag and rebound action potentials on injection of a hyperpolarizing current pulse (Fig. 1B) and showing a prominent voltage-dependent delay in initiation of the first AP on injection of depolarizing current pulses (Fig. 1C; see also Min et al., 2008), were used for subsequent voltage clamp mode (VCM) recordings. Furthermore, the recorded neurons needed to be DBH-ir, as shown by *post hoc* IHC (Fig. 1A). In general, we found that neurons with a large somatic diameter (~ 25 μm) and displaying the above mentioned firing and membrane properties were all DBH-ir.

Outward currents were evoked in NAergic A7 neurons by stepping the Vm from -90 to 0 mV. The currents quickly reached a peak, then decayed rapidly to a sustained level of about 40% of the peak amplitude (Fig. 2Ai). Bath application of 10 mM 4-aminopyridine (4-AP) dramatically reduced the peak amplitude, but did not affect the sustained component of the evoked currents (Fig. 2B). The IC_{50} for the inhibitory effect of 4-AP on the peak amplitude was ~1.4 mM (Fig. 2C; n = 10 cells). These results showed that the evoked outward currents were a mixture of I_A, which showed 4-AP-sensitivity and fast activation/inactivation, and delay rectifier potassium currents (I_{DR}), which were 4-AP-insensitive, slowly activated, and did not show inactivation. The estimated E_r of I_A were -64.6 ±1.2 mV (n = 5 cells; Fig. 2D), a value consistent with that reported in cortical pyramidal neurons (-68.7 mV, Bekkers, 2000). The deviation of E_r of I_A from the theoretical equilibrium potential of K^+ in our recording condition (~106 mV) might be because the potassium channels mediating I_A are also slightly permeable to Na^+ (Sah et al., 1988). Voltage stepping from -40 mV to 0 mV only evoked the non-inactivated I_{DR} (Fig. 2Ai), and subtraction of this current from that evoked on stepping from -90 mV to 0 mV yielded the fast activated/inactivated I_A (Fig. 2Aii). Superimposing I_A with 4-AP sensitive currents shows consistency of kinetics, including the rise and decay phases (Fig. 2B). The mean peak amplitude, 10-90% rise time, and

inactivation time constant (τ_{inac}) for the I_A estimated from 10 NAergic A7 neurons were 6.1 ± 0.2 nA, 5.0 ± 0.2 ms, and 61 ± 3 ms, respectively. To test whether the inactivation rate of the I_A depended on the Vm, 50 mM TEA was added to the bath medium to completely block I_{DR}, and I_A were evoked by voltage steps from -100 mV to various voltage level. As shown in Fig. 3F, there was no significant increase in the τ_{inac} of the I_A on increasing the voltage step used (Fig. 3F), showing no dependence of I_A inactivation on the Vm.

Figure 3A and B show representative recording from two NAergic A7 neurons, showing the I_A evoked by pulses stepped to different voltage levels (A) and by a pulse preceded by different pre-pulse voltage levels (B). The peak conductance and peak amplitude of the I_A in (A) and (B) were measured and used to construct the activation and inactivation curve, respectively. Figure 3C shows the steady state activation/ inactivation curves for the I_A averaged from 6 and 7 NAergic A7 neurons, respectively. The threshold for I_A activation was between -60 to -50 mV. The half-point and slope factor were -18.9 ± 3.1 mV and 12.1 ± 0.9 mV, respectively, for the activation curve (see dotted line in Fig. 3C) and -72.3 ± 2.3 and 7.0 ± 0.3 mV, respectively, for the inactivation curve (Figure 3C, solid line). The activation and inactivation curves overlapped at a Vm between -60 and -30 mV (see insert in Fig. 3C). The recovery of the I_A from inactivation was very rapid, with a $\tau$of 21.9 ± 2.8 ms (Fig. 3D & E). Taken together, the above results show that the I_A in NAergic A7 neurons have properties of fast activation/inactivation, fast recovery from inactivation, a voltage- independent inactivation rate, and sensitivity to 4-AP, with an IC_{50} of 1.4 mM.

The I_A in DBH-ir neurons in the A7 area is mediated by Kv 4.1 and Kv4.3 channels

The above dynamic properties of the I_A suggested that it might be mediated by Kv4 channels. To test this possibility we examined the effect on the I_A of α-dendrotoxin (α-DTX) or BDS-1, specific blockers of Kv1 and Kv3 channels, respectively (Diochot et al., 1998; Dodson et al, 2002). Neither 250 nM DTX (Fig. 4B) nor 1 μM BDS-1 (Fig. 4C) had a significant effect on the I_A (96.7 ± 3.3 % and 97 ± 4 % of control levels for BDS-1 and -DTX, respectively, in Fig. 4D; n = 3 cells tested in each case). In contrast,

application of heteropodatoxin-2 (Hptx-2), a specific Kv4 channel blocker (Sanguinetti et al., 1997; Ramakers and Strom, 2002), significantly reduced the I_A to 61.4 ± 6.1 % of control levels (n = 4 cells tested; P < 0.01, paired t-test) (Fig. 4A & D). These pharmacological results showed that Kv4 channels are involved in the generation of the I_A in NAergic A7 neurons.

We next employed IHC to examine which Kv4 channel subtypes are expressed in NAergic A7 neurons. TH-ir neurons in the A7 area were stained with anti-Kv4.1 channel antibody (Fig. 5A). In addition, they showed clusters of Kv4.3 channel-ir structures on the membrane of the soma and proximal dendrites (Fig. 5C). These stained patterns were not seen when the anti-Kv4.1 or Kv4.3 channel antibodies were omitted during staining procedures (Fig. 5D) or when anti-Kv4.2 channel antibody was used (Fig. 5B). It is unlikely that the negative staining seen using anti-Kv4.2 channel antibody was due to poor quality antibody, as the granule cell layer of the cerebellum, in which Kv4.2 channel expression has been well demonstrated (Wang and Schreurs, 2006; Shibata et al., 1999), was strongly stained by the same antibody (data not shown). The same staining results were obtained in all 4 animals examined. These results therefore suggest a role for Kv4.1 and Kv4.3 channels, but not Kv4.2 channels, in mediating the I_A in NAergic A7 neurons.

The I_A plays important roles in action potential shape and firing pattern in DBH-ir neurons in the A7 area

Using CCM recording, blocking the I_A with Hptx-2 caused a significant increase in the half-width of the AP (control vs. Hptx-2: 3.8 ± 0.3 vs. 4.5 ± 0.5 ms, n = 5 neurons; p < 0.05, paired t-test), but did not affect the amplitude of the AP (control vs. Hptx-2: 109 ± 3 vs. 111 ± 3 mV, n = 5 neurons; p < 0.05, paired t-test) (Fig. 6A1). Similar results were obtained when 4-AP was used; the AP half-width was increased from 3.7 ± 0.3 ms in the control to 4.6 ± 0.4 ms after 4-AP application (n = 7 neurons; p < 0.05, paired t-test), while the AP amplitude was 110 ± 3 mV in the control and 113 ± 2 mV in the presence of 4-AP (n = 7 neurons; p > 0.5, paired t-test) (Fig. 6A2). These results show that the I_A probably accelerates AP repolarization in NAergic A7 neurons. To confirm this possibility, we examined the activation of the I_A using the AP-clamp protocol. As shown in the green trace in Fig. 6Bi, I_m were evoked by a voltage

command of a single AP waveform recorded in CCM (black trace in Fig.6Bii), and this effect was reduced by bath application of 4-AP (red trace in Fig. 6Bi). Subtraction of the I_m recorded in 4-AP from that in the control medium yielded the 4-AP-sensitive current (blue trace in Fig.6Bii), which was presumed to be the I_A. Superimposition of the subtracted I_A on the AP waveform (Fig6Bii) revealed that activation of the I_A started during the repolarization phase of the AP and reached its peak when the AHP was about to develop (indicated by the gray shaded rectangle), showing that I_A were indeed involved in the acceleration of AP repolarization and contributed to the AHP.

Addition of Hptx-2 also significantly reduced the delay in resumption of spontaneous firing on turning off the hyperpolarizing current pulse and significantly increased the inter-spike frequency (Fig. 7A&B). Similar, but larger, effects were seen when 10 mM 4-AP was used. These results show that I_A might be activated by a sub-AP threshold voltage to prolong the inter-AP interval, thereby decreasing the firing frequency of NAergic A7 neurons. To test this possibility, the subthreshold voltage change between 2 consecutive APs during spontaneous firing was used for VCM recording. As shown in Fig. 7C, a 4-AP-sensitive current, presumed to be the I_A, was induced by the inter-AP voltage change, the peak amplitude of which, averaged from 6 A7 NAergic neurons, was 25±5 pA.

The I_A plas important roles in EPSC integration in DBH-ir neurons in the A7 area

Since the Kv4.3 channel has been reported to be involved in synaptic integration (Kim et al, 2007), we next examined whether it played a similar role in NAergic A7 neurons by testing whether an EPSP voltage command could evoke I_A. We first confirmed that the locally-evoked synaptic activity (EPSC) was mediated by both non-NMDA and NMDA receptors in voltage clamp recording using the non-NMDA receptor inhibitor DNQX and the NMDA receptor inhibitor APV (Fig. 8A). We next recorded EPSP activity in CCM and used the EPSP waveform as the voltage command to evoke I_A in the same NAergic A7 neurons. As shown in Fig. 8B, a 4-AP-sensitive current, presumed to be the I_A, was again induced, showing that the EPSP spreading from the dendritic area to soma was able to activated I_A in NAergic A7 neurons. In line with this observation, bath application of 10 mM 4-AP caused a robust

augmentation of EPSP activity in the CCM recording. In the presence of 4-AP, APs were frequently elicited, which was rarely seen in the control condition (Fig. 8C). As shown in Fig. 8D, in the VCM recording, 4-AP also augmented the EPSC by increasing its peak amplitude and broadening its half-width, and this was associated with a reduction in the paired-pulse ratio. Nevertheless, the enhancing effect of 4-AP on synaptic transmission could be due not only to its blocking I_A in recorded neurons, but also to inhibiting other potassium channels located on the presynaptic terminals, thereby enhancing transmitter release as indicated by an increased paired-pulse ratio. To confirm the role of I_A in synaptic integration, we tested the effect of 4-AP on an artificial EPSP (aEPSP) elicited by air-puffed glutamate. We first confirmed that this aEPSP activity was mediated by both non-NMDA and NMDA receptors; a typical experiment is shown in Fig. 8Ei and similar results were obtained in all 3 NAergic A7 neurons tested. To test the effect of 4-AP, the pressure and duration of the air-puff were adjusted so that the puffed glutamate depolarized the Vm to an level at which an averaged number of 3.3 ± 0.6 spikes was evoked per applied air-puff of glutamate (Fig. 8Eii, upper traces). The latency between the start of the air-puff and the onset of the first AP and the slope of the aEPSP rise phase were measured and the averaged values were found to be 1103 ± 259 ms and 286 ± 45 mV/s (n = 5 cells), respectively. Application of 4-AP increased the spike number to 7 ± 0.9 and the slope to 486 ± 44 mV/s and decreased the latency to 623 ± 158 ms ($p<0.01$ for each case, paired-t test). These results are consistent with those for synaptic stimulation (Fig. 8C) and confirmed that the I_A play an important role in modulation of synaptic integration in NAergic A7 neurons.

四、討論

In this study we demonstrated that fast activated and inactivated I_A could be consistently evoked in NAergic A7 neurons. The kinetic properties and the pharmacological profiles of the I_A in NAergic A7 neurons resembled those previously reported for Kv4-mediated currents. In line with these observations, IHC staining showed that NAergic A7 neurons expressed Kv4.1 and Kv4.3 channels. Blockade of the I_A using 4-AP or Hptx-2 increased the half-width and frequency of APs and increased EPSP activity in NAergic A7 neurons. Voltage clamp recording using the waveform of a single AP, a subthreshold voltage

change between 2 consecutive APs, or EPSP activity evoked I_A activity, showing that the I_A play important roles in speeding up AP repolarization, tuning the AP frequency, and promoting synaptic integration in NAergic A7 neurons.

Of the voltage-dependent K^+ channels, the Kv1.4, Kv3.4, and Kv4 channel subfamilies are putative α-subunits (pore-forming subunits), which are responsible for the fast activation/inactivation I_A in various types of neurons (Coetzee et al., 1999; Jerng e al., 2004a). Our argument for a role of Kv4.1/Kv4.3 channels in NAergic A7 neurons is based on the gating properties and pharmacological profiles of the I_A recorded in these neurons. First, the I_A induced in NAergic A7 neurons displayed a voltage-independent inactivation rate, which distinguishes the I_K mediated by Kv4 channels from those mediated by other K^+ channels (Jerng et al., 2004a). Although small differences were noted, the half-points and the slopes of the activation/inactivation curves, the time constants of inactivation, and the recovery from inactivation of the I_A in NAergic neurons were all compatible with the values reported for Kv4.2 or Kv4.3 channels in other neurons in the central nervous system (CNS), including hippocampal pyramidal cells and interneruons (Martina et al., 1998), midbrain dopaminergic neurons (Liss et al., 2001), neurons in the medial nucleus of the trapezoid body (Johnston et al., 2008), and cerebellar granule cells (Shibata et al., 2000). In these studies, the fact that the I_A were mediated by Kv4.3 or Kv4.2 channels was proved by experiments that either showed a positive correlation between the current density of the I_A and the amount of Kv4 channel transcription or block of the I_A by specific knock down of Kv4 channel function. The slight differences in the estimated gating parameters between the present study and these previous studies might stem from the spacing clamping problem of whole-cell recording from NAergic A7 neurons, which have a large somatic diameter and complicated dendritic arborization (Min et al., 2008). It might be also attributed to the differential expression of auxiliary subunits in addition to Kv4 channels in different types of CNS neurons, as these auxiliary subunits have been shown to modulate the gating properties of voltage-dependent K^+ channels (An et al., 2000; Jerng et al., 2004b, 2005). Taken together, the features of the I_A recorded in NAergic A7 neurons, including the relatively low threshold for activation, fast inactivation, rapid recovery from inactivation, and the voltage-independent inactivation

rate, all favor a role of Kv4 channels, and not Kv1 or Kv3 channels, in mediating the I_A. The I_A recorded in NAergic A7 neurons was not affected by application of -DTX and BDS-1, selective blockers of Kv1 and Kv3 channels (Diochot et al., 1998; Dodson et al, 2002), but was significantly attenuated by Heptx-2, a selective Kv4 channel blocker (Sanguinetti et al., 1997; Ramakers and Storm, 2002). These pharmacological results provide further support for a role for Kv4 channels in mediating the I_A. In agreement with the results of these pharmacological and physiological studies, IHC staining results showed that NAergic A7 neurons express Kv4.1 and Kv4.3 channels, but not Kv4.2 channels.

The feature of a low activation threshold makes Kv4 channels an ideal molecular device for regulating the AP frequency in CNS neurons, including NAergic A7 neurons. The AP of NAergic A7 neurons is followed by a prominent AHP (see Fig. 1), which could facilitate the de-inactivation of Kv4 channels, thereby allowing them to operate at a subthreshold Vm. The lowest point of the AHP and the AP threshold in NAergic A7 neurons were about -65 and -40 mV, respectively (see Fig. 5C), which is within the activation window of the I_A (~ -70 to -30 mV), defined as the overlap of the steady state activation and inactivation curves. It is therefore likely that, during spontaneous firing, a substantial percentage of Kv4.1/4.3 channels are able to operate when the Vm is below the threshold for an AP, and that these subthreshold-operating Kv4 channels play a part in regulating the spiking frequency. Indeed, a 4-AP-sensitive current, presumed to be the I_A, was evoked by voltage command using the waveform of the voltage change between 2 consecutive APs during spontaneous firing.

Using EPSP activity as the voltage command also evoked a 4-AP-sensitive outward current, suggesting that Kv4 channels located on the somatic and proximal dendritic membranes play a role in synaptic integration (see also Kim et al., 2007; Ramakers and Storm 2002). Activation of the I_A by EPSP activity would require a much stronger synaptic strength to initiate APs in neurons that express Kv4 channels (such as NAergic A7 neurons), as a substantial proportion of the synaptic current will be counteracted by the I_A when the EPSP spreads toward the soma. This argument was confirmed by the present results showing that initiation of an AP was delayed when the Vm was depolarized to the AP

threshold with an air-puff of glutamate and that blocking the I_A using 4-AP dramatically reduced this delay. In addition, the slope of the aEPSP was also increased, showing that blockade of the I_A using 4-AP increased synaptic current injection during the rise phase of the aEPSP. In NAergic A7 neurons, both non-NMDA and NMDA receptors contribute to the EPSP and aEPSP. Blocking the Kv4 channels means that no I_A is generated and no synaptic current is needed to counteract it, thereby resulting in more rapid and greater depolarization and the activation of a greater number of NMDA receptors. Because the time-course of NMDA receptor currents are significantly longer than those of non-NMDA receptor currents, the activation of the former allows more efficient temporal summation of synaptic inputs and the accommodation of more spikes. All of these features support the idea that the I_A are important in synaptic integration in NAergic A7 neurons.

NAergic A7 neurons receive several neuropeptidergic inputs from descending nuclei, such as substance P released by axonal inputs from the PAG and lateral hypothalamus. Substance P has been reported to activate a non-selective cation current through the neurokinin-1 receptor (Min et al, 2008, 2009). As suggested by the present results, the excitatory effect of substance P on NAergic A7 neurons would not only cause membrane depolarization, but also increase spiking frequency and the efficacy of excitatory synaptic integration by inactivating Kv4 channels. In particular, the function of Kv4 channels can be regulated by phosphorylation by signal cascades activated by neurotransmitters or modulators (Yuan et al., 2002; Chen et al., 2006), allowing more efficient regulation of neuronal spiking and excitability. For example, it is well established that, in chronic pain animals, there is increased extracellular signal-regulated kinase (ERK) activity in various brain regions that are involved in nociceptive signal perception and modulation, including the dorsal spinal cord and central amygdala (Ji et al., 1999, 2003; Wei et al., 2006; Carrasquillo and Gereau, 2007), and it was recently reported that this increased ERK activity downregulates Kv4.2 channel function by phosphorylating the Kv4.2 channel, which increases the excitability of dorsal horn neurons and facilitates the transmission of nociceptive signals (Hu et al., 2002; 2006).

It has been shown that NA exerts a biphasic effect on pain modulation. Behavioral tests show that activation of $_2$ adrenoceptors produces anti-nociceptive effects, while activation of $_1$ adrenoceptors in the dorsal horn of the spinal cord results in hyperalgesia (Nuseir and Proudfit, 2000; Holden and Naleway, 2001). Since NA has a higher affinity for $_2$ receptors than $_1$ receptors (Ramos and Arnsten, 2007), the concentration profile of NA in the dorsal horn would determine the effect (analgesia or hyeralgesia) exerted by NA in the dorsal horn. Given that axons of NAergic A7 neurons are one of the principal source of NAegic innervation in the dorsal spinal cord in rats (Clark and Proudfit, 1991; Kwiat and Basbaum, 1992), a change in spiking frequency or pattern of NAergic A7 neurons would directly reflect a change in the local NA concentration profile in the dorsal spinal cord, thereby altering the nociceptive signaling regulation function of NA. In conclusion, the present results show that I_A mediated by Kv4.1/Kv4.3 channels play important roles in regulating firing frequency and synaptic integration in NAergic A7 neurons and that modulating the function of these channels can change the firing frequency of NAergic neurons, which might alter the pain regulation function of NA in the dorsal horn of the spinal cord.

一、 參考文獻

An WF, Bowlby MR, Betty M, Cao J, Ling HP, Mendoza G, Hinson JW, Mattsson KI, Strassle BW, Trimmer JS, Rhodes KJ (2000), Modulation of A-type potassium channel by a family of calcium sensors. Nature 403:553-556.

Barbaro NM, Hammond DL, Fields HL (1985), Effects of intrathecally administrated methysergide and yohimbine on microstimulation produces antinociception in the rat. Brain Res 343:223-229.

Bekkkers JM (2000), Properties of voltage-gated potassium currents in nucleated patches from layer 5 cortical pyramidal neurons of the rats. J Physiol 525:593-609.

Burdakov D, Ashcroft FM (2002), Cholecystokinin tunes firng of an electrically distinct subset of arcuate nucleus neurons by activating A-type potassium channels. J Neurosci 22:6380-6387.

Burdakov D, Alexopoulos H, Vincent A, Ashcroft FM (2004), Low-voltage-activated A-current controls the firing dynamics of mouse hypothalamic orexin neurons. Eur J Neurosci 20:3281-3285.

Carlsson A, Falck B, Fuxe K, Hillarp NA (1964), Cellular localization of monoamines in the spinal cord. Acta Physiol Scand 60:112-119.

Carrasquillo Y, Gereau RW (2007), Activation of the Extracellular signal- regulated kinase in the Amygdala Modulates Pain Perception. J Neurosci 27:1543–1551.

Chen X, Yuan L-L, Zhoa C, Birnbaum SG, Frick A, Jung WE, Schwarz TL, Sweatt JD, Johnston D (2006), Deletion of Kv4.2 gene eliminates dendritic A-type K^+ current and enhances induction of long-term potentiation in hippocampal CA1 pyramidal neurons. J Neurosci 26:12134-12151.

Clark FM, Proudfit HK (1991), The projection of noradrenergic neurons in the A7 catecholamine cell group to the spinal cord in the rat demonstrated by anterograde tracing combined immunohistochemistry. Brain Res 547:279-288.

Coetzee WA, Amarillo Y, Chiu J, Chow A, Lau D, McCormack T, Moreno H, Nadal MS, Ozaita A, Pountney D, Saganich M, Vega-Saenz de Miera E, Rudy B. (1999),The molecular diversity of K^+ channels. Ann NY Acad Sci 868:233-285.

Dahlsötrm A, Fuse K (1964), Evidence for the existence of monoamine- containing neurons in the central nervous system. I. Demonstration of monoamines in the cell bodies of brain stem neurons. Acta Physiol Scand 62 Suppl 232:1-55.

Danzebrink RM, Gebhart GF (1990), Antinociceptive effects of intrathecal adrenoceptor agonists in a rat model of visceral nociception. J Pharmacol Exp Ther 253:698–705.

Dias QM, Crespilho SF, Silveria WS, Prado WA. (2009), Muscarinic and a1-adrenergic mechanisms contribute to the spinal mediation of stimulation-induced antinociception from the pedunculopotine tegmental nucleus in the rat. Pharmacol Biochem Behav 92:488-494.

Diochot S, Schweitz H, Beress L, Lazdunski M (1998), Sea anemone peptide with a specific blocking activity against the fast inactivating potassium channel Kv3.4. J Biol Chem 273:6744-6749.

Dodson PD, Barker MC, Forsythe ID (2002), Two heteromeric Kv1 potassium channels differentially regulate action potential firing. J Neurosci 22:6953-6961.

Hodge CJ, Apkarian AV, Stevens RT (1986), Inhibition of dorsal horn cell response by stimulation of the Kölliker-Fuse nucleus. J Neurosurg 65: 825-833.

Holden JE, Naleway E (2001), Microinjection of carbachol in the lateral hypothalamus produces opposing actions on nociception mediated by α1 and 2-adrenoceptors. Brain Res 911:27-36.

Holden JE, Pizzi JA (2003), The challenge of chronic pain. Adv Drug Deliv Rev 55:935-948.

Holden JE, Schwartz EJ, Proudfit HK (1999), Microinjection of morphine in the A7 catecholamine cell group produces opposing effects on nociception that are mediated by alpha1- and alpha2-adrenoceptors. Neuroscience 83:979–990.

Howorth PW, Teschemacher AG, Pickering AE (2009), Retrograde adenoviral vector targeting of nociresponsive pontospinal noradrenergic neurons in the rat in vivo. J Comp Neurol 512:141-157.

Hu H-J, Glauner KS, Gereau RW (2002), ERK integrates PKA and PKC signaling in superficial dorsal horn neurons. I. Modulation of A-type K^+ currents. J Neurophysiol 90 :1671-1679.

Hu H-J, Carrasquillo Y, Karim F, Jung WE, Nerbonne JM, Schwarz TL, Gereau RW (2006), The Kv4.2 potassium channel subunit is required for pain plasticity. Neuron 50:89-100.

Jerng HH, Pfaffinger PJ, Covarrubias M (2004a), Molecular physiology and modulation of somatodendritic A-type potassium chanels. Mol Cell Neurosci 27:343-369.

Jerng HH, Oian Y, Pfaffinger PJ (2004b), Modulation of Kv4.2 channel expression and gating by dipeptidyl peptidase 10 (DPP10). Biophysic J 87:2380-2396.

Jerng HH, Kunjilwar K, Pfaffinger PJ (2005), Multiprotein assembly of kv4.2, KchIP3 and DPP10 produces ternary channel complexes with ISA-like properties. J Physiol 568:767-788.

Ji RR, Baba H, Brenner GJ, Woolf CJ (1999), Nociceptive-specific activation of ERK in spinal neurons contributes to pain hypersensitivity. Nat. Neurosci 2: 1114-1119.

Ji RR, Kohno T, Moore KA, Woolf CJ (2003), Central sensitization and LTP: do pain
and memory share similar mechanisms? *Trends Neurosci.* **26**, 696-705.

Johnston J, Griffin SJ, Baker C, Forsythe ID (2008), Kv4 (A-type), potassium currents in the mouse medial nucleus of the trapezoid body. Eur J Neurosci 27:1391-1399.

Jones SL (1991), Descending noradrenergic influences on pain. Prog Brain Res 88, 381–394.

Kim J, Jung SC, Clemens AM, Petralia RS, Hoffman DA (2007), Regulation of dendritic excitability by activity-dependent trafficking of the A-type K+ channel subunit Kv4.2 in hippocampal neurons. Neuron 57:933-947.

Kuraishi Y, Hirota N, Satoh M, (1985) Antinociceptive effects of intrathecal opioids, noradrenaline and serotonin in rats: mechanical and thermal algesic tests. Brain Res 326:168–171.

Kwiat GC, Basbaum AI (1992), The origin of brainstem noradrenergic and serotonergic projections to the spinal cord dorsal horn in the rat. Somatosens Mot Res 9:157–173.

Liss B, Franz O, Sewing S, Bruns R, Neuhoff H, Roeper J (2001), Tuning pacemaker frequency of individual dopaminergic neurons by Kv4.3L and KChip3.1 transcription. EMBO J 20:5715- 5724.

Martina M, Schultz JH, Ehmke H, Monyer H, Jonas P (1998), Functional and molecular differences between voltage-gated K^+ channels of fast-spiking interneurons and pyramidal neurons of rat hippocampus. J Neurosci 18:8111-8125.

Millan MJ (1999), The induction of pain: an integrative review. Prog Neurobilo **57**:1-164.

Millan MJ (2002), Descending control of pain. *Prog Neurobiol* 66:355-474.

Min M-Y, Hsu P-C, Yang H-W (2003), The physiological and morphological characteristics of interneurons caudal to the trigeminal motor nucleus in rats. Eur J Neurosci 18:2981-2998.

Min M-Y, Wu Y-W, Shih P-Y, Lu H-W, Lin C-C, Wu Y, Li M-J, Yang H-W (2008), Physiological and morphological properties of, and effect of Substance P on, Neurons in the A7 Catecholamine Cell Group in Rats. Neuroscience 153 :1020-1033.

Min M-Y, Shih P-Y, Wu Y-W, Lu H-W, Lee M-L, Yang H-W et al. (2009), Neurokinin 1 receptor activates transient receptor potential-like currents in noradrenergic A7 neurons in rats. Mol Cell Neurosci 42:56-65.

Neher E (1992), Correction for liquid junction potential in patch clamp experiments. Methods Enzymol 207:123-131.

Nuseir K, Proudfit HK (2000), Bidirectional modulation of nociception by GABA neurons in the dorsolateral pontine tegmentum that tonically inhibit spinally projecting noradrenergic A7 neurons. Neuroscience 96:773-783.

Pertovaara A (2006), Noradrenergic pain modulation. Prog Neurobiol 80:53-83.

Ramakers GMJ, Storm JF (2002), A postsynaptic transient K^+ current modulated by arachidonic acid regulates synaptic integration and threshold for LTP induction in hippocampal pyramidal cells. Proc Natl Acad Sci USA :10144-10149.

Ramos BP, Arnsten AF (2007), Adrenergic pharmacology and cognition: focus on prefrontal cortex. Pharmacol Ther 113:523-536.

Reddy SV, Yaksh TL (1980), Spinal noradrenergic terminal system mediates antinociception. Brain Res 189:391–401.

Sagen J, Proudfit HK (1981), Hypoalgesia induced by blockade of noradrenergic projections to the raphe magnus: reversal by blockade of noradrenergic projections to the spinal cord. Brain Res 223:391-396.

Sah P, Gibb AJ, Gage PW (1988) Potassium currents activated by depolarization in dissociated neurons from adult guinea pig hippocampus. J Gen. Physiol. 92:263-278.

Sanguinetti MC, Johnson JH, Hammerland LG, Kelbaugh PR, Volkmann RA, Saccomano NA, Mueller AL (1997), Heteropodatoxins: peptides isolated from spider venom that block Kv4.2 potassium channels.

Mol Pharmacol 51:491-498.

Satoh M, Oku R, Akaike A (1983), Analgesia produced by microinjection of L-glutamate into the rostral ventromedial bulbar nuclei of rats and its inhibition by intrathecal adrenergic blocking agents. Brain Res 261:361-364.

Shibata R, Wakazono Y, Nakahira K, Trimmer JS, Ikenaka K (1999), Expression of Kv3.1 and Kv4.2 genes in developing cerebellar granule cells. Dev Neurosci 21:87-93.

Shibata R, Nakahira K, Shibasaki K, Wakazono Y, Imoto K, Ikenaka K (2000), A-type K^+ current mediated by the Kv4 channel regulates the generation of action potential in developing cerebellar granule cells. J Neurosci 20:4145-4155.

Takano Y, Yaksh TL (1992), Characterization of the pharmacology of intrathecally administered a2 agonists and antagonists in rats. J Pharmacol Exp Ther 261:764–772.

Wang D, Schreurs BG (2006), Characteristics of IA currents in adult rabbit cerebellar Purkinje cells. Brain Res 22:85-96.

Wei F, Vadakkan KI, Toyoda H, Wu LJ, Zhao MG, Xu H, Shum FW, Jia YH, Zhuo M (2006), Calcium calmodulin-stimulated adenylyl cyclases contribute to activation of extracellular signal-regulated kinase in spinal dorsal horn neurons in adult rats and mice. J Neurosci 26:851-861.

Wu Y-W (2007). Functional role of A-type potassium channels in A7 catecholamine cell group in rats. Master Thesis.

Yeomans DC, Proudfit HK (1992), Antinociception induced by microinjection of substance P into the A7 catecholamine cell group in the rat. Neuroscience 49:681-691.

Yeomans DC, Clark FM, Paice JA, Proudfit HK (1992), Antinociception induced by electrical stimulation of spinally-projecting neurons in the A7 catecholamine cell group of the rat. Pain 48:449-461.

Yuan LL, Adams JP, Swank M, Sweatt JD, Johnston D (2002), Protein kinase modulation of dendritic K+ channels in hippocampus involves a mitogen-activated protein kinase pathway. J Neurosci 22:4860-4868.

六、圖與圖說

圖一

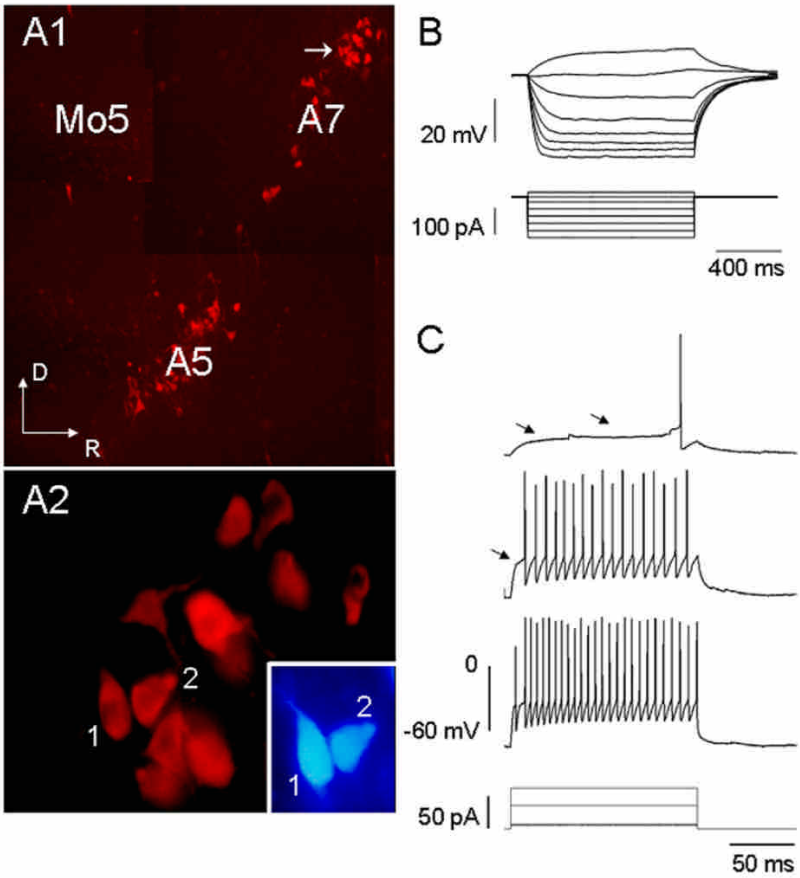

Fig. 1. Recordings from, and membrane properties of, NAergic A7 neurons. (A) Fluorescent microscopy photograph showing results of DBH immunostaining and biocytin–avidin D-AMCA histochemistry performed on a brainstem slice after electrophysiological recording. In (A1), the two groups of DBH-ir neurons located rostral and ventral to Mo5 are the A7 and A5 catecholamine cell groups, respectively. In (A2) two neurons (labeled "1" and "2") in the A7 area were recorded and filled with biocytin (insert) and were confirmed as NAergic, as both were DBH-ir. (B, C) Transmembrane voltage responses to hyperpolarizing (B) or suprathreshold (C) current injections in an NAergic A7 neuron (cell "1" in A2). Note there is no voltage sag or rebound AP when a large hyperpolarizing current is injected (B) and there is a significant delay in the first AP on injection of a suprathreshold depolarizing current (see arrows in C). For interpretation of the references to color in this figure legend, the reader is referred to the Web version of this article.

圖二

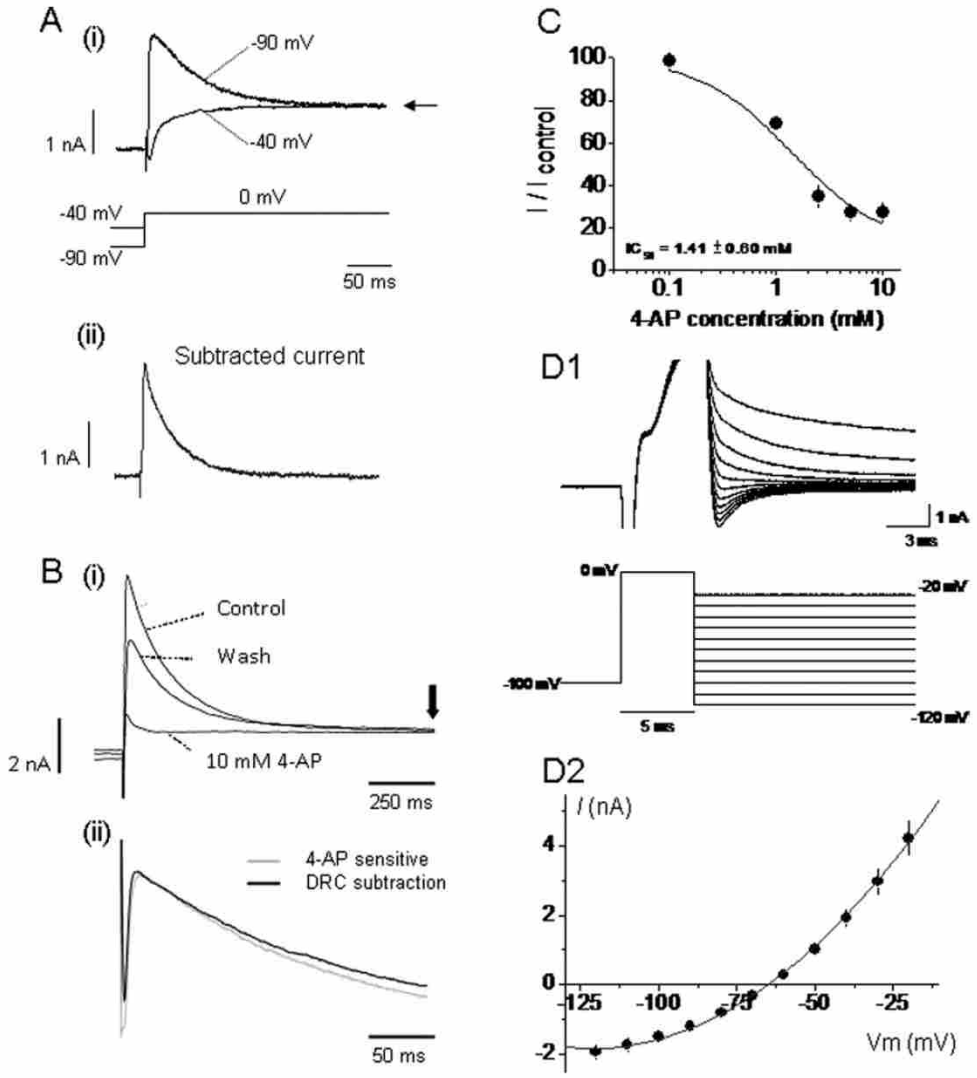

Fig. 2. Recording of the I_A in NAergic A7 neurons. (A) Effect of a voltage step from −90 to 0 mV or from −40 to 0 mV (Ai). Subtraction of the I_m evoked by the voltage step with a pre-pulse voltage of −40 mV from that evoked with a pre-pulse voltage of −90 mV yields the fast activated and inactivated I_A (Aii). (B) The peak amplitude of the I_m evoked by a voltage step from −90 mV is largely attenuated by application of 10 mM 4-AP, while the sustained part of the membrane current is not affected (see arrow) (Bi). Subtraction of currents recorded in 4-AP from those recorded in control, yields 4-AP sensitive currents (grey trace in Bii), which is superimposed with I_A obtained by subtracting currents evoked by the voltage step from −40 to 0 mV from those evoked by the voltage step from −100 to 0 mV (black trace in Bii). Amplitude of traces shown in (Bii) were normalized. (C) The reduction by 4-AP of the peak amplitude of the I_m evoked by a voltage step from −90 to 0 mV is dose-dependent. The effect of 0.1, 1, 2.5, 5, and 10 mM 4-AP was tested in four, six, four, five, and eight NAergic A7 neurons, respectively. (D) Superimposed tail currents of I_A (upper traces) evoked by voltage steps from −100 to 0 mV (5 ms), followed to a level ranging from −20 to −120 mV with 10 mV increments (lower traces) (D1). The peak amplitude of tail currents was measured and plotted versus voltage level (D2). Data were fitted to a quadratic polynomial equation (solid line).

圖三

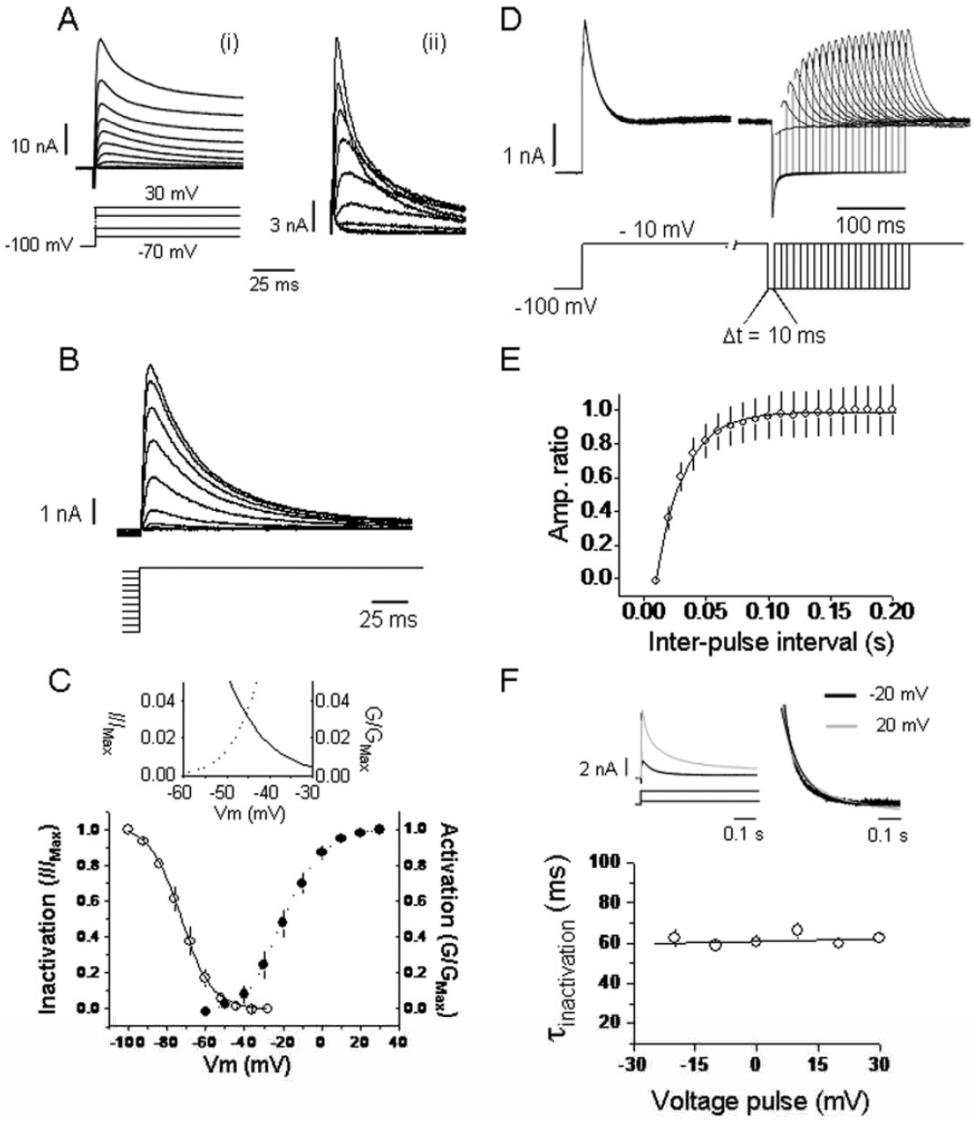

Fig. 3. Gating properties of the I_A in NAergic A7 neurons. (A) Superimposed I_m (i) and I_A (ii) evoked in an NAergic neuron (upper traces). The whole-cell I_m were evoked by voltage steps from −70 to +30 mV with a 10 mV increment (lower traces shown in i). Traces of I_A (ii) were obtained by digital subtraction of the currents evoked from a holding of −40 mV from I_m. (B) Superimposed I_A (upper traces) evoked by voltage steps from various pre-pulse voltage levels (−100 to −28 mV with an 8 mV increment) (lower traces) to −10 mV. (C) The activation (white circles+solid line)/inactivation (black circles+dotted line) curve for the I_A, summarized from 10 NAergic neurons. Note the overlapping of the two curves between Vm of ~−30 to −60 mV, as shown in the insert. The solid and dotted lines were obtained by fitting the Boltzmann's equation to the data. (D) Superimposed I_A (upper traces) evoked by paired voltage pulses from −100 to −10 mV with various inter-pulse intervals from 10 to 200 ms with a 10 ms increment (lower traces). (E) The curve of recovery from inactivation summarized from 10 NAergic neurons. The solid line shows the results of fitting single exponential growth to the data. (F) The upper left traces show the I_A evoked by stepping the Vm from −100 mV to −20 (black) or 20 mV (gray), respectively. The upper right traces show the I_A normalized according to the same peak amplitude. Only the decay portions of the currents are shown; the results show that the time course of decay from −20 (black) or 20 mV (gray) are very similar. The lower panel shows summarized results from five NAergic A7 neurons. Note there is no significant increase in the inactivation time constant (τ) with an increase in the voltage level used to evoke I_A, showing that inactivation of I_A is independent of the Vm.

圖四

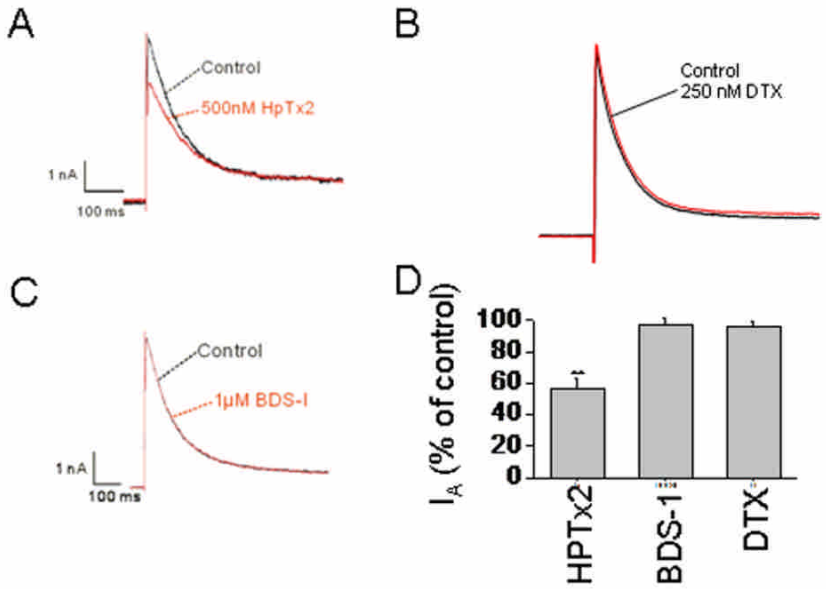

Fig. 4. The I_A are attenuated by a Kv4 channel blocker, but not a Kv1 or Kv3 channel blocker. (A) Representative traces showing the I_A evoked in an NAergic A7 neuron under normal conditions (black) and in the presence of 500 nM HpTx-2 (red), a specific Kv4 channel blocker. (B, C) Representative traces showing the I_A evoked in two NAergic A7 neurons under normal conditions (black) and in the presence (red) of α-DTX, a specific Kv1 channel blocker (B), or BDS-1, a specific Kv3 channel blocker (C). (D) Summarized results for NAergic neurons tested for the effect of Hptx-2 (four neurons), BDS-1 (three neurons), or α-DTX (three neurons). For interpretation of the references to color in this figure legend, the reader is referred to the Web version of this article.

圖五

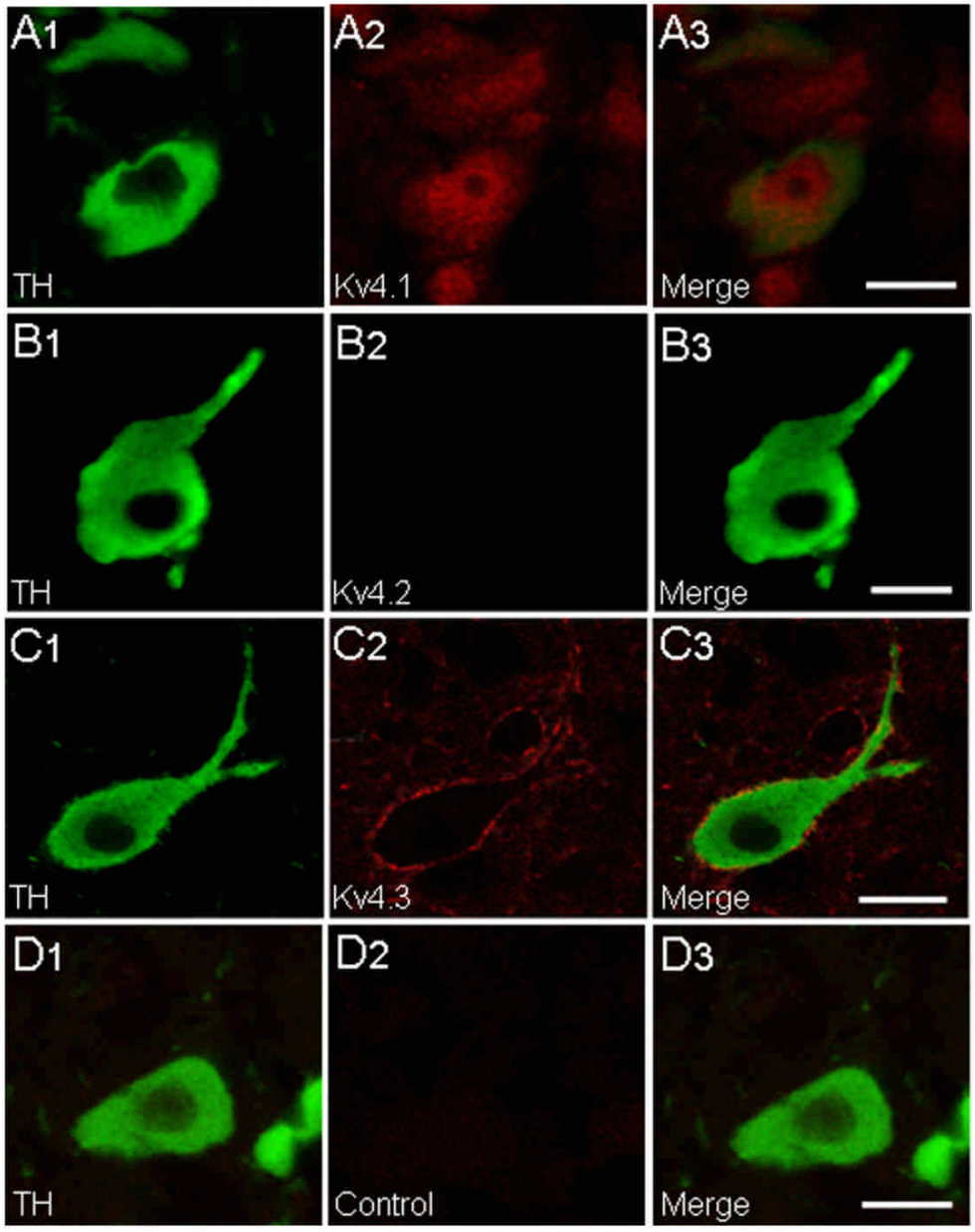

Fig. 5. Expression of Kv4.1 and Kv4.3 channels in NAergic A7 neurons. Results of immunostaining using antibodies against TH and the Kv4.1 channel (A), antibodies against TH and the Kv4.2 channel (B), antibodies against TH and the Kv4.3 channel (C), or antibody against TH alone (D). For interpretation of the references to color in this figure legend, the reader is referred to the Web version of this article.

圖六

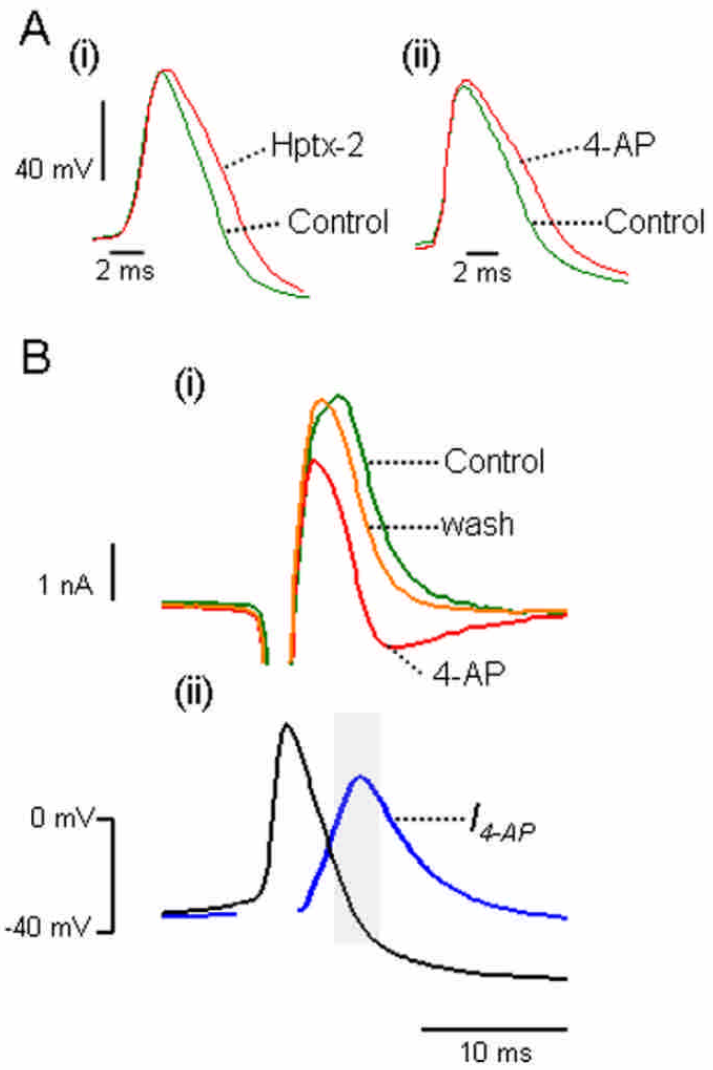

Fig. 6. The I_A contribute to the repolarization and AHP of the AP in NAergic A7 neurons. (A) The half-width of the AP in NAergic neurons is increased by Hptx-2 (i) or 4-AP (ii). (B) A representative AP voltage-clamp experiment. The black trace in (ii) is the AP recorded in CCM. Using this AP waveform as the voltage command for subsequent VCM recording evoked outward currents (green trace in i) in the same neuron. Application of 4-AP largely reduced the currents (red trace in i); subtraction of the currents recorded under normal conditions from that in the presence of 4-AP revealed the I_A underlying the AP (blue trace in ii), showing that the I_A are mainly evoked during the repolarizing phase and AHP of the AP, as indicated by the gray shaded rectangle. For interpretation of the references to color in this figure legend, the reader is referred to the Web version of this article.

圖七

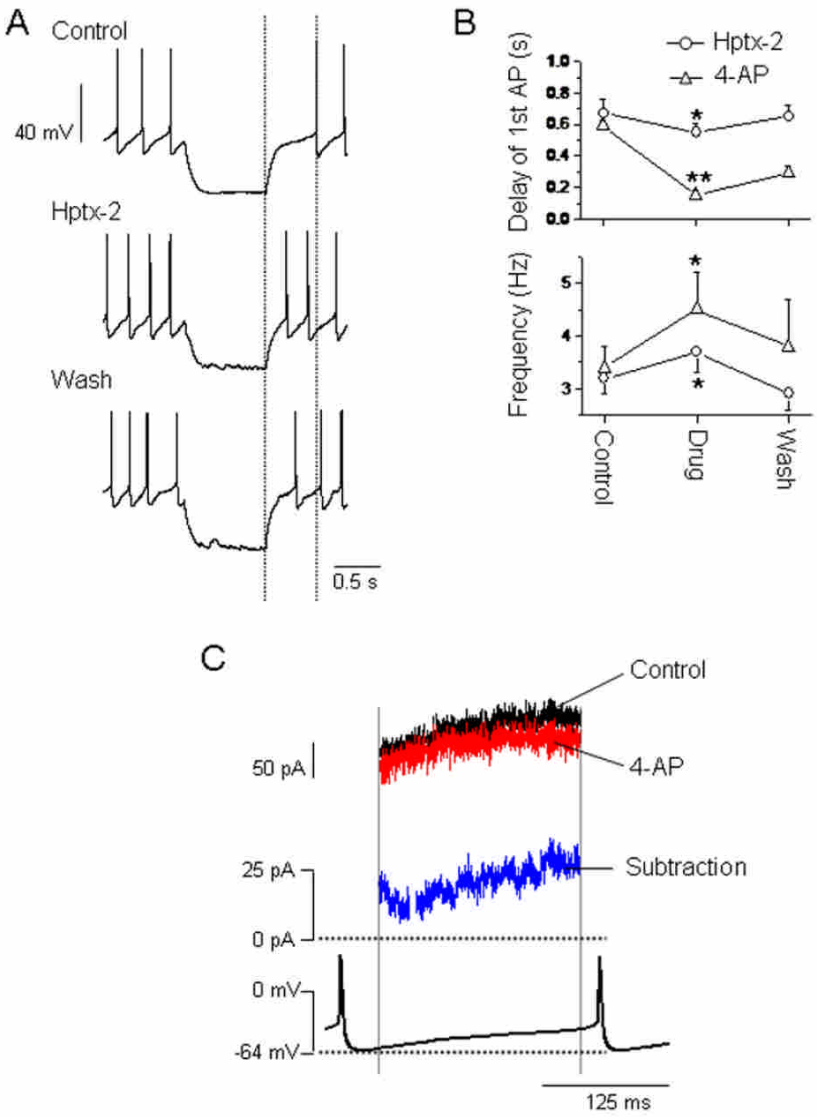

Fig. 7. The I_A are involved in tuning the AP frequency in NAergic A7 neurons. (A) CCM recording from an NAergic A7 neuron in control conditions (top trace) or in the presence of Hptx-2 (middle trace) and wash of Hptx-2 (bottom trace). Note the reduced AP interval on application of Hptx-2 and the recovery on washout of the drug. Injection of a hyperpolarizing current pulse delays the onset of AP (indicated by dotted lines) which was blocked by Hptx-2. (B) Summarized results showing that Hptx-2 or 4-AP significantly reduces the delay to the first AP and increases the AP frequency in NAergic neurons. Four NAergic neurons were tested for the effect of Hptx-2 and five for the effect of 4-AP. (C) A representative VCM recording experiment using the voltage change between two APs as the voltage command. The black trace in the lower panel shows the APs recorded in CCM. The black trace in the upper panel shows the I_m evoked using the voltage change between two APs as the voltage command in the same neuron. Application of 4-AP dramatically reduces the I_m (red trace) and subtraction of the I_m recorded in the presence of 4-AP from that in control conditions reveals the I_A (blue trace), which is activated during the subthreshold voltage change between two APs. For interpretation of the references to color in this figure legend, the reader is referred to the Web version of this article.

圖八

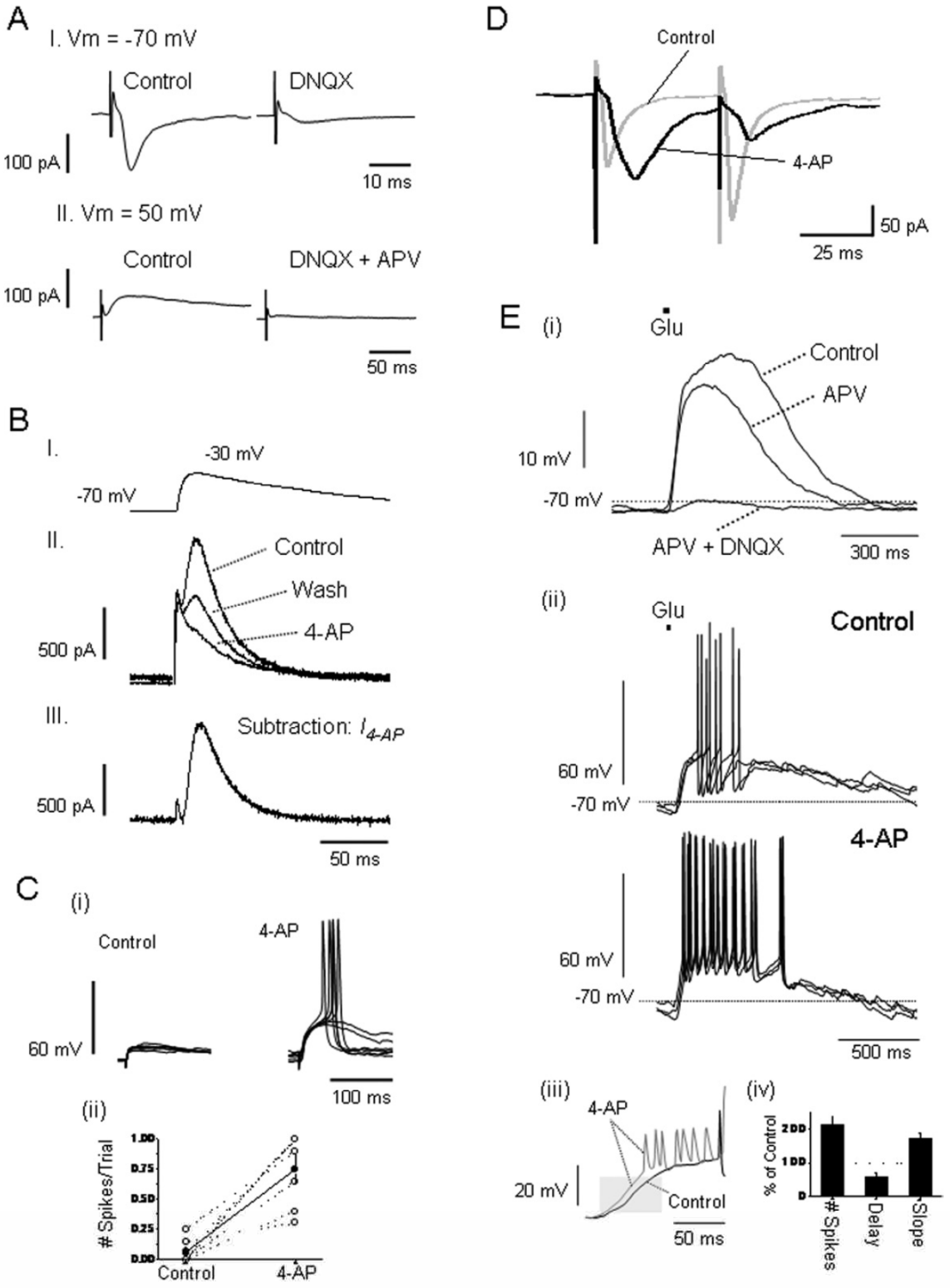

Fig. 8. The I_A play a role in modulating synaptic integration in NAergic A7 neurons. (A) Recording and elicitation of EPSC activity by a local bipolar stimulating electrode in an NAergic A7 neuron. The upper trace shows the EPSC activity averaged from 20 consecutive sweeps with the Vm clamped at −70 and its blockade by DNQX. Lower trace: Outward synaptic currents were revealed in the same neuron when the Vm was subsequently clamped at +50 mV and were completely blocked by further application of APV. (B) A representative VCM experiment using the EPSP activity as the voltage command. The top trace is the averaged EPSP from 100 consecutive sweeps in CCM recording. Using this EPSP activity as the voltage command evokes an outward I_m (middle trace) in subsequent VCM recording in the same neuron. Application of 4-AP dramatically reduced the I_m, which showed partially recovery after washout of drug; subtraction of the current recorded in the normal condition from that in the presence of 4-AP reveals the I_A

國科會補助專題研究計畫項下出席國際學術會議

心得報告

日期：99年10月27日

計畫編號	NSC 95－2323－B－040－011－MY3		
計畫名稱	大白鼠中腦A7核區正腎上腺素神經元A型鉀離子電流之分子和生理特性分析與角色探討		
出國人員姓名	楊 琇 雯	服務機構及職稱	中山醫學大學 生物醫學科學系
會議時間	2010年7月3日至 2010年7月7日	會議地點	阿姆斯特丹
會議名稱	(中文) 第七屆歐洲神經科學會議 (英文) The 7th forum of European Neuroscience		
發表論文題目	(中文)大鼠A7 catecholamine 細胞的$GABA_B$受器媒介強直抑制作用研究 (英文)$GABA_B$ receptor mediated tonic inhibition in noradrenergic neurons of the A7 catecholamine cell group in rats		

一、參加會議經過

本次會議由本人與其他合作同仁共發表 4 篇壁報論文。其中與此計畫相關的正腎上腺性 A7 神經元研究的論文共計 3 篇，分別於

七月五日下午：

1. Orexin-immunoreactive terminals in the rats A7 area: light- and electron-microscopic analysis of their relationships with noradrenergic neurons

七月六日上午：

2. Cholinergic modulation in A7 noradrenergic neurons
3. $GABA_B$ receptor mediated tonic inhibition in noradrenergic neurons of the A7 catecholamine cell group in rats

二、與會心得

今年第七屆歐洲神經科學會議在荷蘭的首都阿姆斯特丹舉行，約有數千人來自全球的神經科學家參與會議，然而仍以歐洲學界的學者參與居多。從會議中的壁報論文的質與量，可看出歐洲的神經科學水準是相當的高。會議中安排有 plenary lectures， special lectures 與 symposium，因此不論是新的在進行中的研究（如壁報論文）、重要研究主題的回顧與未來展望（symposium 會議），或者歐洲傑出學者的經典研究（如 plenary lectures， special lectures），都能提供與會者非常多的選擇，因此是一個安排很好的會議。本人在此次會議中有幸聆聽許多演講，與有機會與其他與會學者暢談。其中受益最大是是能與瑞士的 Luscher 教授與其實

驗室同仁討論有關，$GABA_B$ receptor 與 GIRK channel 在中樞神經系統的調節功能中，特別是在 Dopamine 與 Norepinephrine 神經元的調控；此外，周邊運動神經的傷害所造成的運動神經元放電行為的改變的 symposium 中，也得到許多因生理或病理刺激下，離子通道種類的改變能引發神經細胞放電行為的截然不同，進而引起神經迴路重大的功能重塑。

國科會補助計畫衍生研發成果推廣資料表

日期:2010/11/04

國科會補助計畫	計畫名稱: 大白鼠中腦A7核區正腎上腺素神經元A型鉀離子電流之分子和生理特性分析與角色探討
	計畫主持人: 楊琇雯
	計畫編號: 95-2320-B-040-011-MY3　　學門領域: 解剖

無研發成果推廣資料

95 年度專題研究計畫研究成果彙整表

計畫主持人：楊琇雯	計畫編號：95-2320-B-040-011-MY3
計畫名稱：大白鼠中腦 A7 核區正腎上腺素神經元 A 型鉀離子電流之分子和生理特性分析與角色探討	

成果項目			量化			單位	備註（質化說明：如數個計畫共同成果、成果列為該期刊之封面故事...等）
			實際已達成數（被接受或已發表）	預期總達成數(含實際已達成數)	本計畫實際貢獻百分比		
國內	論文著作	期刊論文	0	0	0%	篇	
		研究報告/技術報告	0	0	0%		
		研討會論文	0	0	0%		
		專書	0	0	0%		
	專利	申請中件數	0	0	0%	件	
		已獲得件數	0	0	0%		
	技術移轉	件數	0	0	0%	件	
		權利金	0	0	0%	千元	
	參與計畫人力（本國籍）	碩士生	0	0	0%	人次	
		博士生	0	0	0%		
		博士後研究員	0	0	0%		
		專任助理	0	0	0%		
國外	論文著作	期刊論文	2	2	100%	篇	
		研究報告/技術報告	0	0	0%		
		研討會論文	1	1	100%		
		專書	0	0	0%	章/本	
	專利	申請中件數	0	0	0%	件	
		已獲得件數	0	0	0%		
	技術移轉	件數	0	0	0%	件	
		權利金	0	0	0%	千元	
	參與計畫人力（外國籍）	碩士生	0	0	0%	人次	
		博士生	0	0	0%		
		博士後研究員	0	0	0%		
		專任助理	0	0	0%		

其他成果 (無法以量化表達之成果如辦理學術活動、獲得獎項、重要國際合作、研究成果國際影響力及其他協助產業技術發展之具體效益事項等，請以文字敘述填列。)	無

	成果項目	量化	名稱或內容性質簡述
科教處計畫加填項目	測驗工具(含質性與量性)	0	
	課程/模組	0	
	電腦及網路系統或工具	0	
	教材	0	
	舉辦之活動/競賽	0	
	研討會/工作坊	0	
	電子報、網站	0	
	計畫成果推廣之參與（閱聽）人數	0	

國科會補助專題研究計畫成果報告自評表

請就研究內容與原計畫相符程度、達成預期目標情況、研究成果之學術或應用價值（簡要敘述成果所代表之意義、價值、影響或進一步發展之可能性）、是否適合在學術期刊發表或申請專利、主要發現或其他有關價值等，作一綜合評估。

1. 請就研究內容與原計畫相符程度、達成預期目標情況作一綜合評估

■達成目標

□未達成目標（請說明，以 100 字為限）

□實驗失敗

□因故實驗中斷

□其他原因

說明：

2. 研究成果在學術期刊發表或申請專利等情形：

論文：■已發表 □未發表之文稿 □撰寫中 □無

專利：□已獲得 □申請中 ■無

技轉：□已技轉 □洽談中 ■無

其他：(以 100 字為限)

3. 請依學術成就、技術創新、社會影響等方面，評估研究成果之學術或應用價值（簡要敘述成果所代表之意義、價值、影響或進一步發展之可能性）(以 500 字為限)

本計畫的成果已發表 2 篇完整的學術論文於 Neuroscience 期刊，分別在 2008 年的第 153 卷，1020-1033 頁與 2010 年的第 168 卷，633-645 頁發表。在第一篇論文中，我們報告正腎上腺性 A7 神經元與其他鄰近的中間神經元的生理與型態特徵與兩種細胞間可能的突觸連結，此結果為學界首度對正腎上腺性 A7 神經元的系統與完整的電生理學研究。之後在第二篇報告中，我們探討 Kv4 通道蛋白在正腎上腺性 A7 神經元的生理功能角色。我們發現 Kv4 通道蛋白在正腎上腺性 A7 神經元的動作電為波形、自主放電頻率控制、與突觸訊息的整合上，均扮演重要的調節角色。愈來愈多研究報告顯示，Kv4 通道蛋白在中樞神經系統中，對神經細胞也有類似的功能角色，因此本計畫結果更進一步確認 Kv4 通道，在中樞神經系統中的確有控制調節細胞興奮性與修飾突觸傳導的生理功能。由於正腎上腺性 A7 神經元間的神經傳導是內生性下行止痛神經迴路的重要成員，本計畫的成果也是第一次報告，Kv4 通道蛋白在此正腎上腺性下行止痛迴路中有重要的角色。